

Sezione di Catania

INFN/BE-72/3
12 Giugno 1972

V. D'Amico, S. Jannelli, F. Mazzanares and R. Potenza :
 ${}^7\text{Li} + d \rightarrow 2\alpha + n$ REACTION: I) ANALYSIS OF THE
BIDIMENSIONAL SPECTRA.

V. D'Amico, S. Jannelli, F. Mezzanares, and R. Potenza: ${}^7\text{Li} + d \rightarrow 2\alpha + n$
REACTION; I) ANALYSIS OF THE BIDIMENSIONAL SPECTRA. -

ABSTRACT. -

The bidimensional spectra of the reaction ${}^7\text{Li} + d \rightarrow 2\alpha + n$ with three bodies in the final state are analyzed by a method that takes into account in a definite approximation the finite resolving power of the detecting system. Some experimental results on this reaction are then analyzed in the system of the relative coordinates, that seems the most suitable to treat the effects of sequential decays.

1. - INTRODUCTION. -

The reactions with three bodies in the final state have received much attention in the last few years^(1÷8) also because of their importance in the heavy ion reactions⁽¹⁾. The mechanisms that seem involved in the transitions to the continuum of three or more particles are:

- i) the sequential decay at low energies of the incident particles^(1÷4);
- ii) the direct knock-out or the stripping to the continuum, at higher incident energies^(5÷8). However the sequential decay process seems to be present also at these higher energies and to compete with the direct processes^(1, 6, 7).

(x) - This work was supported in part by INFN, CRRN and CSFN & SM.

2.

These reactions have been studied up to now by measuring the energy spectra of one particle, the bidimensional spectra and the angular correlations of two particles. It is however clear that the technique of the bidimensional spectra taken at various angles is the most suitable for a complete analysis of the reactions.

Up to now the results of a reaction with three bodies in the final state have been compared with theory in the laboratory system (LS)^(2, 8÷10). In this case, the identity of two or more particles in the final state complicates somewhat the problem of the theoretical explanation of the data and the singularities in the density of the final states in the LS causes other complications.

In view of these facts it seems simpler to compare the data with theory in the system of the relative coordinates (RCS)⁽¹¹⁾. As is shown in sect. 3.2, when sequential processes are important, that is when the intermediate states can be treated as resonant states^(12, 13), the RCS data show directly the characteristics of these states, allow an easy treatment of the identity of the particles and can allow the separation of the contributions of the different intermediate states to the reaction. The transformation of the data to the RCS is possible whenever the bidimensional spectra of the reaction are available in the LS.

However, before performing the transformation to the RCS it is necessary to devise some method to avoid the singularities in the Jacobians and to correct for the fact that in the plane of the coincident pulses the finite angular resolving power of the detectors results in a loss of the energetic resolving power.

Sect. 3.1 of this paper is devoted to show a method, suitable for this purpose, that allows an easy codification for a computer machine.

In Sect. 3.2 the results of the application of this method to some bidimensional spectra of the ${}^7\text{Li}+d \rightarrow 2\alpha+n$ reaction at $E_d=1.0$ MeV are shown, and the spectra in the RCS are reported, taking into account the identity of the two α -particles in the final state.

The extensive analysis of this experiment will be done in the next paper.

2. - COLLECTION OF THE EXPERIMENTAL DATA. -

We studied the ${}^7\text{Li}+d \rightarrow 2\alpha+n$ reaction, bombarding a target of natural Li with deuterons of $E_d=0.8, 1.0$ and 1.2 MeV. The target thickness was 50 keV at 1.0 MeV. Only some results at $E_d=1.0$ MeV are shown in this paper. The deuterons were accelerated by the Van de Graaf electrostatic generator of the CSFN & SM laboratories in Catania.

The α -particles were detected by surface barrier detectors supplied by ORTEC. With the polar axis fixed in the direction of the incident deuterons, one of the detectors (labelled 1) was placed at a fixed polar angle $\theta_1 = 88,4^\circ$ and azimuth $\phi_1 = 0^\circ$ and the other one (labelled 2) was allowed to rotate between $\theta_2 = 30^\circ$ and $\theta_2 = 150^\circ$ at the azimuth $\phi_2 = 180^\circ$. The distances of the target from the detectors were respectively $d_1 = 14$ cm and $d_2 = 12$ cm. The diameters of the detectors were $\phi_1 = \phi_2 = 5.6$ mm. The pulses of these two detectors were sent through two ORTEC amplification chains to a system of fast-slow coincidence ($\tau = 30$ ns) supplied by COSMIC and to a LABEN 4096 channel analyzer in bidimensional operation mode, controlled by the output pulses of the coincidence system. The output pulses of the detector 1, acting also as a monitor, were counted by a scaler. The whole system was controlled by a device that stopped the runs at a fixed number of pulses counted by the detector 1. The measurements were done varying θ_2 in steps of 2° between 30° and 110° .

Fig. 1 shows some bidimensional spectra as presented at the oscilloscope of the analyzer. As it can be noted, the experimental points lie inside a strip of the $E_1 E_2$ plane, where E_1 and E_2 are the energies respectively measured by the detectors 1 and 2. The distribution of the points is not uniform, showing some peaks at positions depending on the angles.

3. - ANALYSIS OF THE EXPERIMENTAL DATA. -

3.1. - Laboratory system. -

3.1.1. - Kinematic relations. -

Let us consider the reaction $P+T=A_1+A_2+A_3$ where P , T , A_1 , A_2 and A_3 are nuclear particles of masses m_p , m_t , m_1 , m_2 and m_3 respectively.

Let E_p , E_1 and E_2 be the kinetic energies of the particles P , A_1 and A_2 in the laboratory system. The conservation laws give in the non-relativistic case:

$$(1) \quad a_1 E_1 + a_2 E_2 + 2c_1 E_1^{1/2} E_2^{1/2} - 2c_1 E_1^{1/2} - 2c_2 E_2^{1/2} - b = 0$$

where

$$a_1 = m_1 + m_3; \quad a_2 = m_2 + m_3; \quad c_1 = (m_1 m_p E_p)^{1/2} \cos \theta_1;$$

4.

$$c_2 = (m_2 m_p E_p)^{1/2} \cos \theta_2; c_{12} = (m_1 m_2)^{1/2} \cos \theta_{12}; b = m_3 Q + (m_3 - m_p) E_p;$$

$$\cos \theta_{12} = \cos \theta_1 \cos \theta_2 + \sin \theta_1 \sin \theta_2 \cos (\phi_2 - \phi_1);$$

$\theta_1, \theta_2, \phi_1$ and ϕ_2 being the polar and azimuthal angles of A_1 and A_2 in the laboratory system and θ_{12} the relative (polar) angle between A_1 and A_2 .

Eq. (1) represents an ellipse in the $E_1^{1/2} E_2^{1/2}$ plane and its physical points are found in the first quadrant (in fact $E_1^{1/2}$ and $E_2^{1/2}$ are proportional to the magnitudes of the momenta). In the plane $E_1 E_2$ a quartic is generally obtained; it is given by:

$$(2) \quad E_i = (a_{ij} + \sqrt{a_{ij}^2 + a_i b_j})^2 / a_i^2 \quad i \neq j$$

where

$$a_{ij} = c_i - c_{12} E_j^{1/2}; \quad b_j = b + 2c_j E_j^{1/2} - a_j E_j$$

Figs. 2 and 3 show some kinematic curves for the studied reaction. One can see that: a) the ellipses have always one positive intersection with each axis; b) the physical quartics are open curves which start and stop at the tangent points to the axes. These points correspond to those where the ellipses intersect the axes; c) there are two points (inversion points) in which the tangents are parallel to the axes.

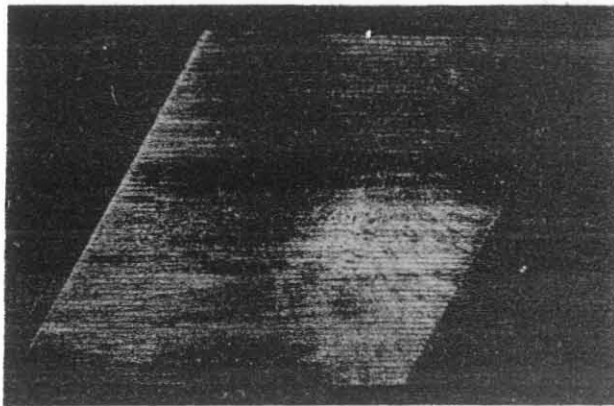
3.1.2. - Bidimensional spectra. -

From that said in sects. 2 and 3.1.1., the particles A_1 and A_2 are those respectively detected by the detectors 1 and 2. The particle A_3 is the undetected particle.

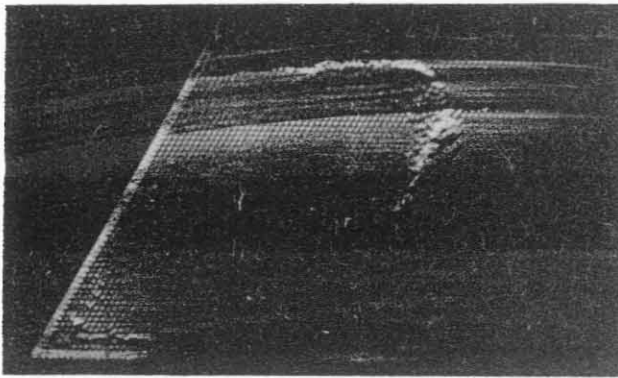
The coincident pulses which A_1 and A_2 give rise to in the detectors cannot lie on a curve of the $E_1 E_2$ plane, but on a narrow strip around the kinematic curve belonging to the given angles of the two detectors and the given energy of the incident particle.

The half-width of this strip depends on the angular spread of the particles and the energy resolution of the detecting and analyzing system. To evaluate this width Δ we have used the expression

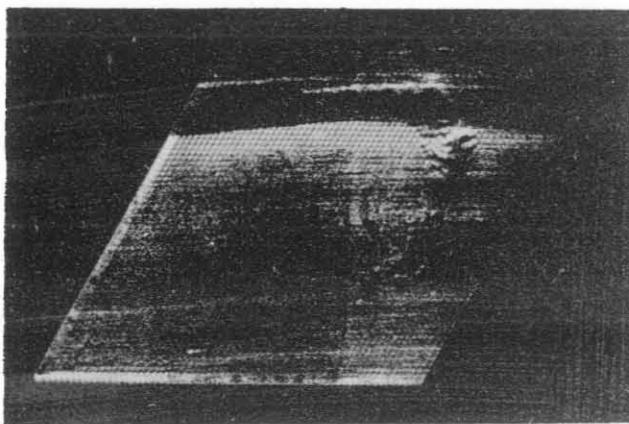
$$(3) \quad \Delta = \sqrt{\Delta l^2 + k(\Delta E)^2}$$



a)



b)



c)

FIG. 1 - Bidimensional spectra of the ${}^7\text{Li}(d, 2a)$ reaction at $E_d = 1.0$ MeV, $\theta_1 = 88.4^\circ$, $\phi_2 - \phi_1 = 180^\circ$;
a) $\theta_2 = 60^\circ$; b) $\theta_2 = 70^\circ$; c) $\theta_2 = 74^\circ$.

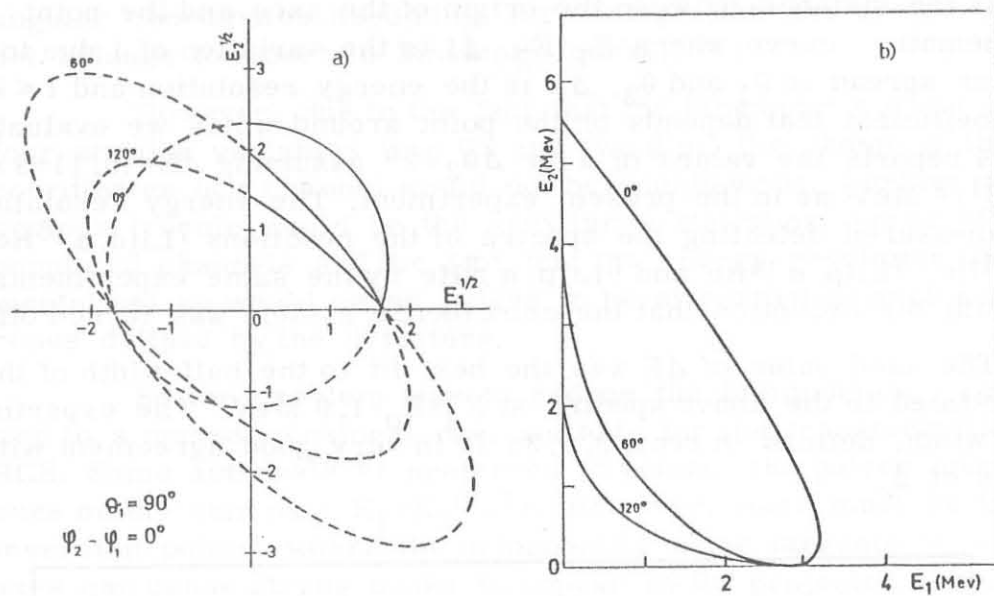


FIG. 2 - Kinematic curves of the ${}^7\text{Li}(d, 2\alpha)$ reaction at $\phi_2 - \phi_1 = 0^\circ$; a) ellipses in the momentum plane); b) corresponding quartics in the energy plane. The dashed parts of the curves are the unphysical parts.

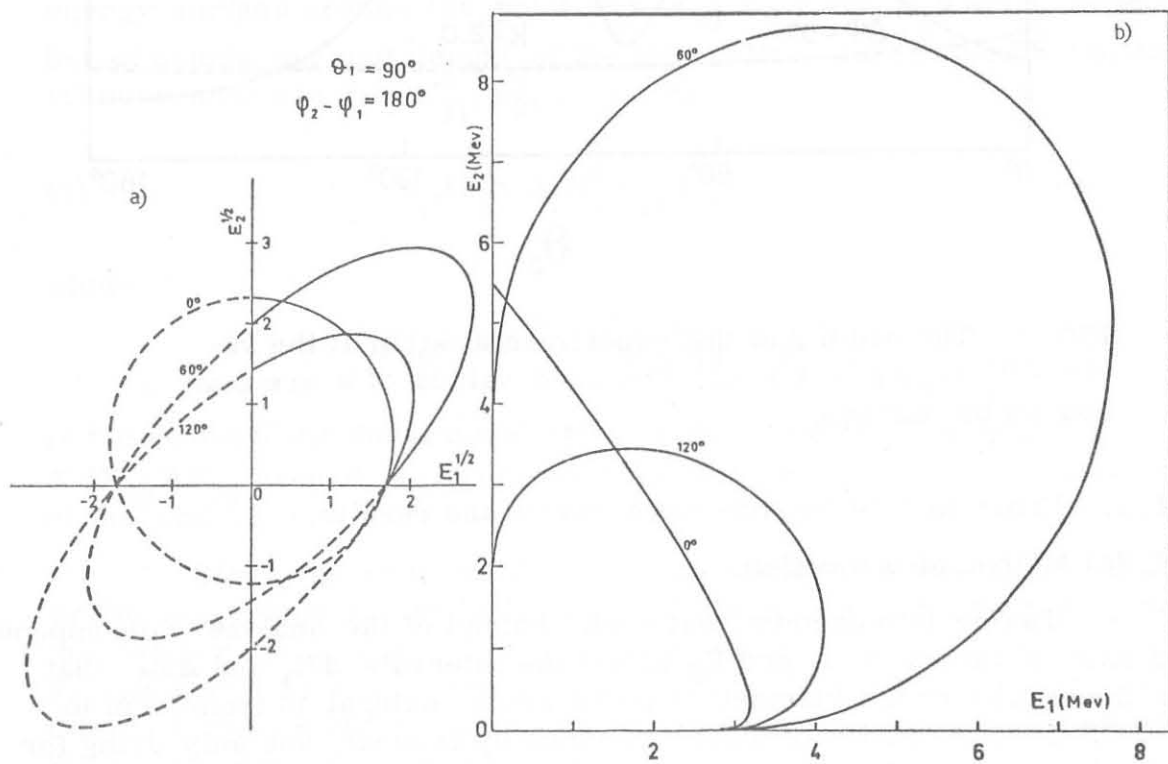


FIG. 3 - As in Fig. 2 at $\phi_2 - \phi_1 = 180^\circ$.

8.

$$(5) \quad N_i^S \Delta s_i = \sum_j N_j P'_{ji} \Delta S_j$$

where P'_{ji} is now the probability that, if a count found in ΔS_j then it belongs to the interval Δs_i around s_i .

We assumed

$$(6) \quad P'_{ji} = \frac{k_j}{\delta_{ji}^2 + \Gamma^2/4} \quad \text{if} \quad \delta_{ji} \leq \Gamma$$

$$P'_{ji} = 0 \quad \text{if} \quad \delta_{ji} > \Gamma \quad \sum_i P'_{ji} = 1$$

where k_j are the normalization constants and $\delta_{ji}^2 = (E_{1j} - E_{1i}^S)^2 + (E_{2j} - E_{2i}^S)^2$.

The use of this method results in smoothing somewhat the experimental data.

In rough approximation this smoothing extends to a circle of radius Γ with weights that decrease going away from the centre. It is clear that there would be no smoothing if P_{ij} and P'_{ij} were unitary matrices. This would be possible only if the data lay in a very small neighbourhood of the kinematic curve and interested a strip of only one file of channels, being in this case P_{ij} diagonal.

In this hypothesis the projection would have been unnecessary and the transformation to the RCS could have been performed channel by channel.

The strip width Γ was chosen at the various angles equal to the first multiple of 0.15 MeV greater than Δ (see sect. 3.1.2). The value of 0.15 MeV corresponds about to the half width of a channel. This choice was tested for various angles counting the number of the pulses selected by the computer around the kinematic curve for various values of Γ in steps of 0.15 MeV. The chosen values resulted those for which a further increase in Γ of 0.15 MeV introduced only a fraction $\approx 2\%$ of new pulses. Fig. 5 shows the significant strip of the $E_1 E_2$ plane selected by the computer at $\theta_2 = 74^\circ$. The value of Γ was 0.6 MeV (see Fig. 4).

3.1.3b) Chance coincidences. -

It was possible to extract the average number of chance coincidences per channel from the parts of the bidimensional spectra out-

side the significant strip populated by the true coincidences.

We observed that the actual number of counts in a large region outside the strip had a Poisson distribution, and computed the average value N_c .

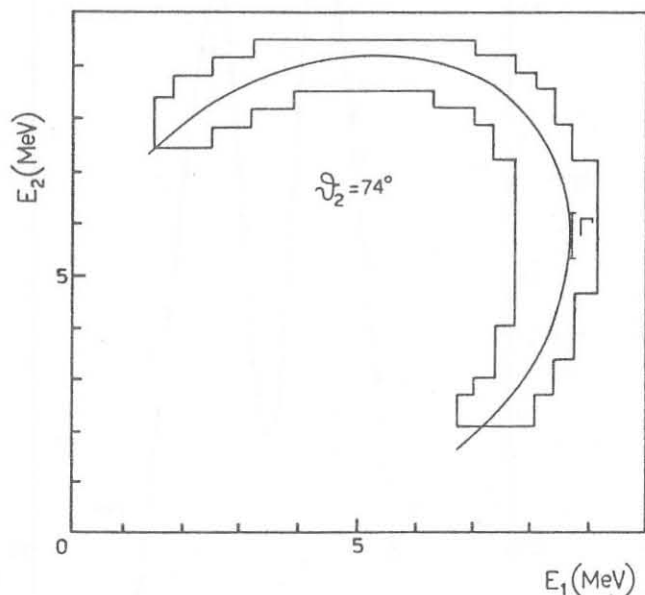


FIG. 5 - The strip in the energy plane selected by the method underlined in the text at $\theta_2 = 74^\circ$. $\Gamma = \Delta$ is the width of the strip.

The number of these chance coincidences was in most spectra of the order of $N_c = 2 \div 3$ and this contribution was subtracted from the counts inside the significant strip after weighing with the use of the spectrum of the particles detected by a single counter.⁽²⁾

3.1.3c) Results. -

Fig. 6 shows the $N(s)$ density vs. the curvilinear abscissa s in the laboratory system at $\theta_2 = 60^\circ, 70^\circ, 74^\circ$. The origins of the curvilinear abscissas are placed at the points where the kinematic curves are tangent to the E_1 axis. The curves are run in counterclockwise sense. The errors are only statistical. The energy resolution coincides with Γ .

3.1.3d) Intrinsic errors of the method. -

One of the most important sources of errors in the projection method outlined in sect. 3.1.3a) seems to be the uncertainty in choosing the kinematic curve over which to project. The choice of this curve is somewhat arbitrary and in fact is a matter of simplicity. So it is useful to see which are the variations in the density $N(s)$ (see section 3.1.3a) when we choose other kinematic curves inside the strip.

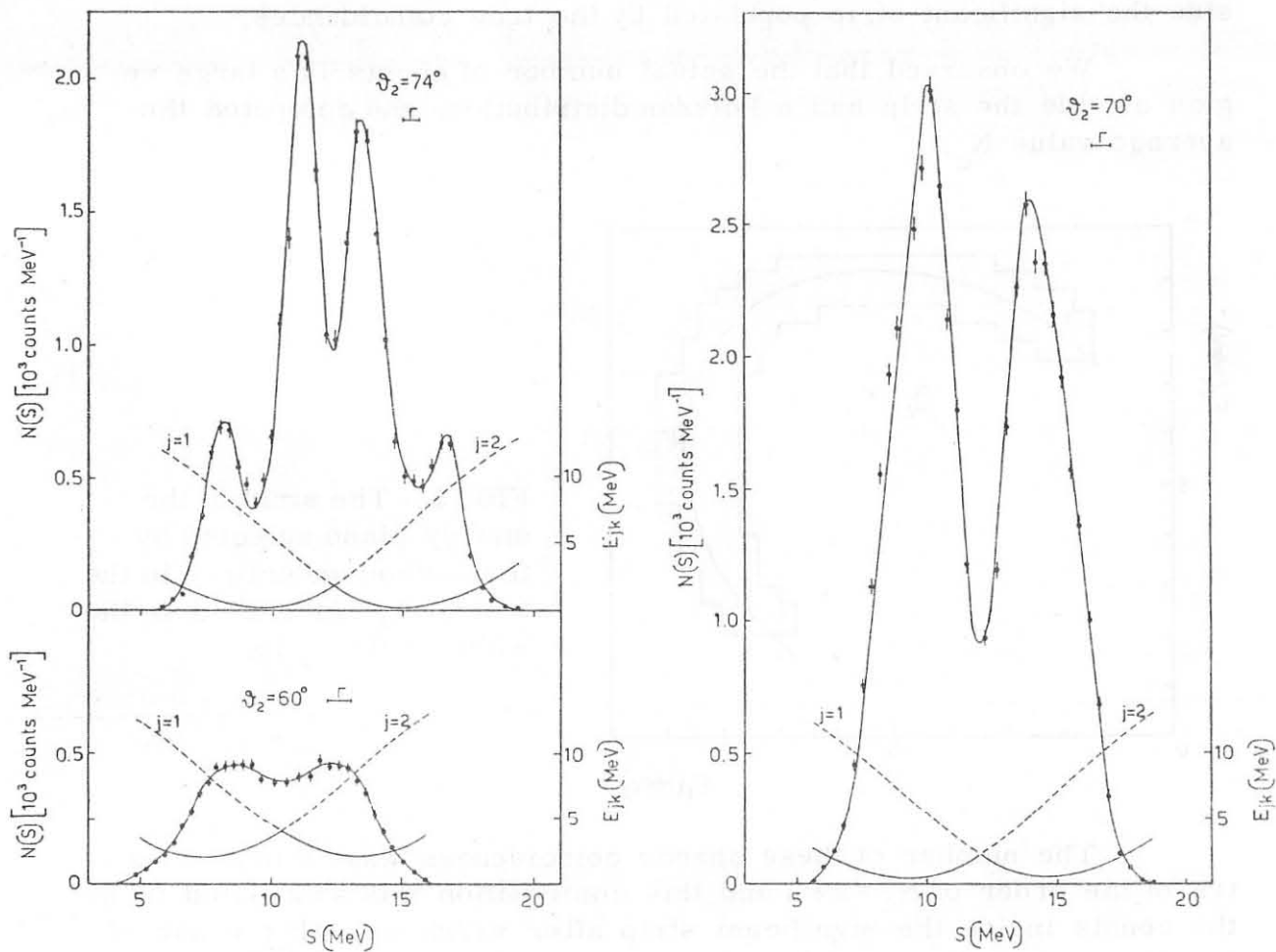


FIG. 6 - The points give the experimental density $N(s) \propto \frac{d^3\sigma}{ds d\Omega_1 d\Omega_2}$ vs. s , the curvilinear abscissa along the kinematic curve. The curves labelled $j=1$ and $j=2$ respectively give E_{j-k} vs. s for $k=3$. The full parts of these last curves refer to the used values of E_{j-k} in the transformation to the RCS. The values of θ_2 are given on the drawings.

We varied the θ_2 angle of the kinematic curve of $\Delta\theta_2 = \pm 1^\circ$ obtaining new sets of $N(s)$ points. The difference between the various sets were rather less than the statistical errors, so we concluded that the method did not introduce appreciable errors.

3.2.- Relative coordinates system (RCS).-

We define the relative coordinates by the well known relations used in ref. (11)

$$(7) \quad \vec{R} = (m_1 \vec{r}_1 + m_2 \vec{r}_2 + m_3 \vec{r}_3) / M$$

$$(7') \quad \vec{r}_{i-jk} = \vec{r}_i - (m_j \vec{r}_j + m_k \vec{r}_k) / (m_j + m_k)$$

$$(7'') \quad \vec{r}_{j-k} = \vec{r}_j - \vec{r}_k$$

for $i \neq j \neq k$; $i, j, k = 1, 2, 3$ and $M = m_1 + m_2 + m_3$. The values 1, 2 and 3 of the indices correspond respectively to the particles A_1, A_2 and A_3 (see sect. 3.1.1. and 3.1.2.). There are, of course, as rels. (7), (7') and (7'') show, several ways of choosing the RCS. The most convenient system is to be suggested by the actual reaction one is studying. In this respect, rel. (7') is the most important to fix the sequential process that is selected by the transformation. The particles labelled j and k are in fact those involved in the second stage of the selected decay. So, in the case of the ${}^7\text{Li} + d \rightarrow 2\alpha + n$, if 2 and 3 refer respectively to an alpha and a neutron, the selected process is that involving the ${}^5\text{He}$ states.

3.2.1. - Relative energies and Jacobian of the transformation. -

The conjugate momenta are

$$(8) \quad \vec{p}_\alpha = \mu_\alpha \vec{V}_\alpha \quad \alpha \equiv i-jk \text{ or } j-k$$

where μ_α and \vec{V}_α are the reduced mass and the relative velocity associated with the relative coordinate \vec{r}_α . The associate kinetic energies are

$$(9) \quad E_\alpha = \frac{p_\alpha^2}{2\mu_\alpha}$$

where E_{j-k} is the internal energy of the system $j-k$.

In terms of rels. (8) we have

$$(10) \quad \frac{P^2}{2M} + \frac{p_{i-jk}^2}{2\mu_{i-jk}} + \frac{p_{j-k}^2}{2\mu_{j-k}} = \frac{p_1^2}{2m_1} + \frac{p_2^2}{2m_2} + \frac{p_3^2}{2m_3} = E_p + Q$$

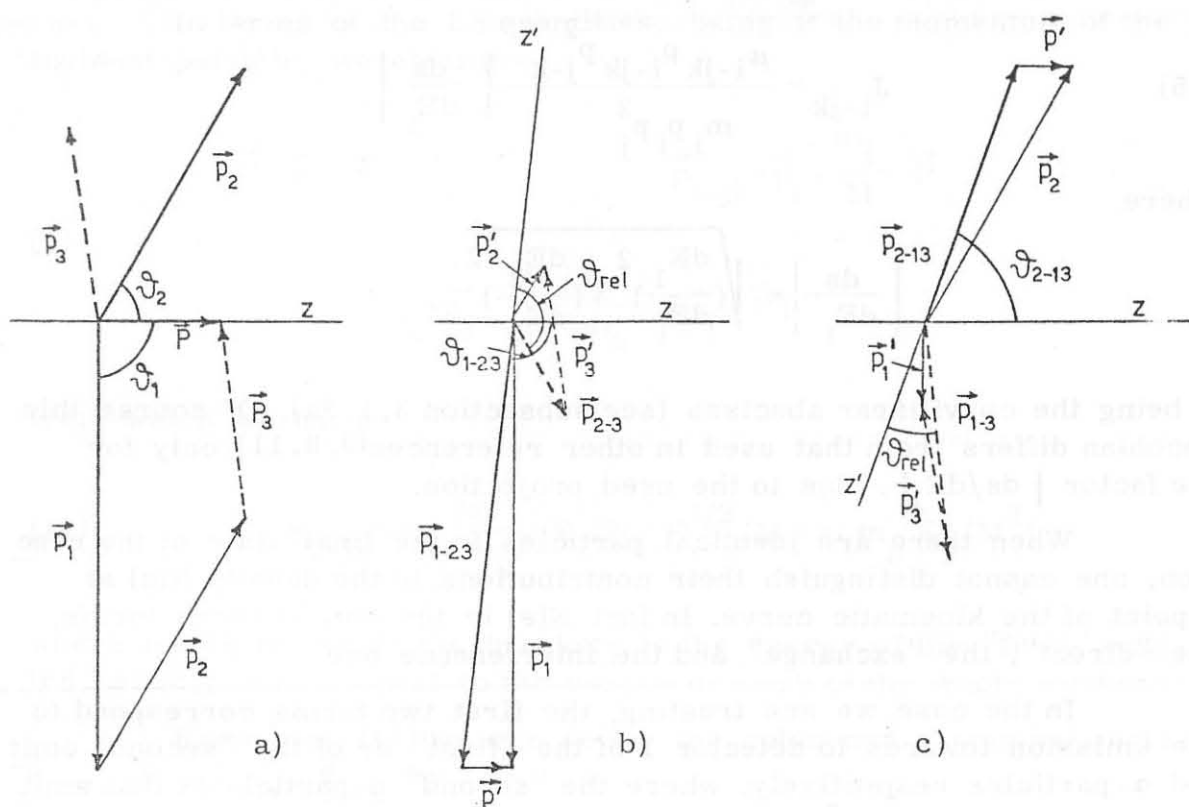


FIG. 7 - Momentum diagrams for the ${}^7\text{Li} + d \rightarrow 2\alpha + n$ reactions, showing the polar axes and the polar angles in the RCS. a) Laboratory system: $\vec{p}_1 + \vec{p}_2 + \vec{p}_3 = \vec{P}$.

b) "Direct" situation in the RCS: the "first" emitted α -particle is that detected by the detector 1.

$$\text{So } \vec{p}_{1-23} = \vec{p}_1 - \frac{m_1}{M} \vec{P} \equiv \vec{p}_1 - \vec{p}' \quad \text{and} \quad \vec{p}_{2-3} = \frac{\mu_{2-3}}{m_2} \vec{p}_2 - \frac{\mu_{2-3}}{m_3} \vec{p}_3$$

$$\vec{p}_{2-3} \equiv \vec{p}'_2 - \vec{p}'_3.$$

c) "Exchange" situation in the RCS: the "first" emitted α -particle is that detected by the detector 2.

$$\text{So } \vec{p}_{2-13} = \vec{p}_2 - \frac{m_2}{M} \vec{P} \equiv \vec{p}_2 - \vec{p}' \quad \text{and} \quad \vec{p}_{1-3} = \frac{\mu_{1-3}}{m_1} \vec{p}_1 - \frac{\mu_{1-3}}{m_3} \vec{p}_3$$

$$\vec{p}_{1-3} \equiv \vec{p}'_1 - \vec{p}'_3.$$

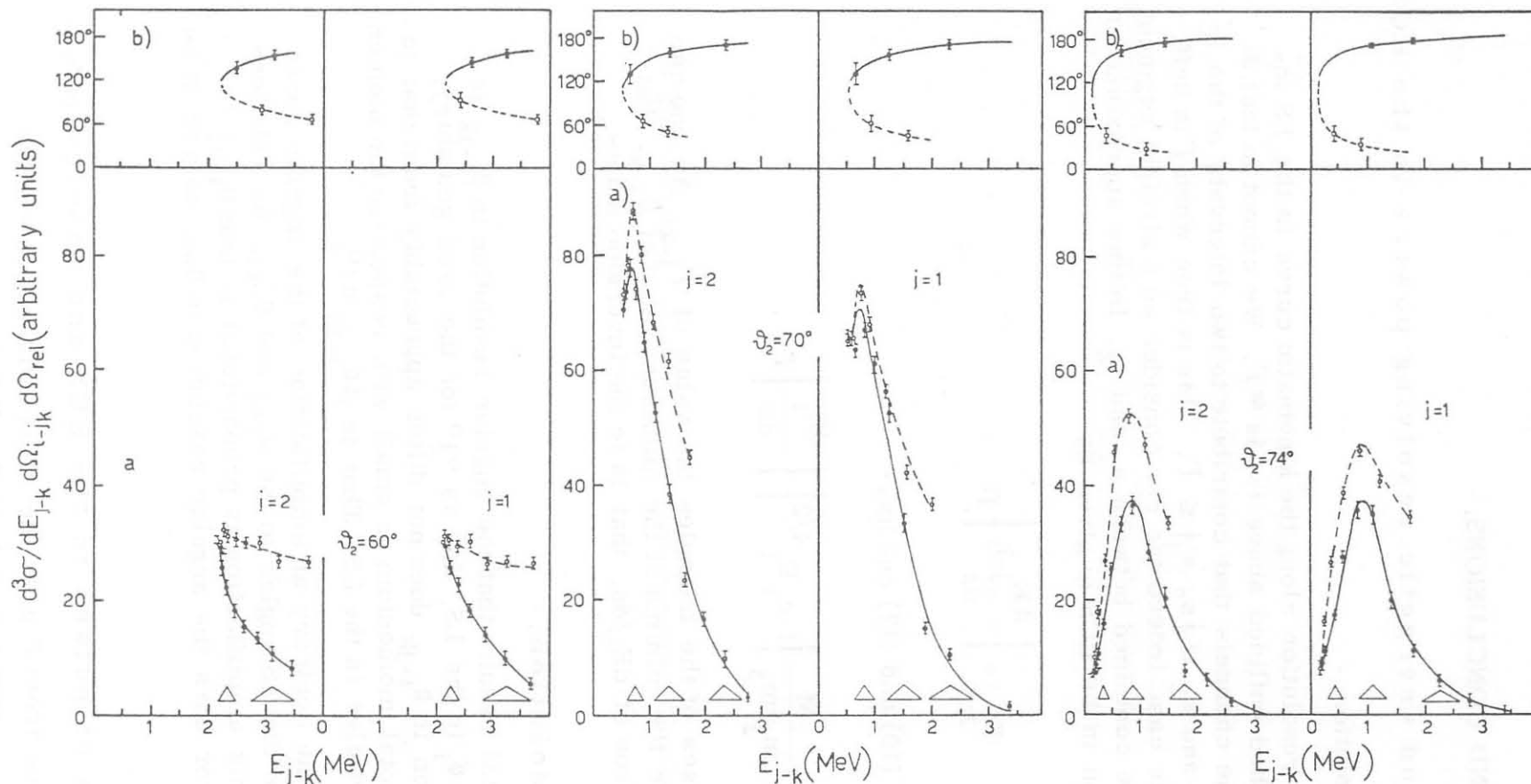


FIG. 8 - a) $d^3\sigma/dE_{j-k} d\Omega_{i-jk} d\Omega_{rel}$ for $i=1,2$ and $j=2,1$ respectively for the spectra shown in Fig. 1. The values of j are reported on the curves. The bases of the triangles give the energy resolution Γ_{j-k} . b) θ_{rel} vs. E_{j-k} . The bars give the angular resolution. The full curves refer to the extremities of the kinematic curves; the dashed ones to the central part of those curves.

4. - DISCUSSIONS AND CONCLUSIONS. -

4.1. - Angular and energetic resolving powers in the RCS.

4.1.1. - Energy resolution. -

The energy resolution along the kinematic curve in the LS introduced by the method outlined above is $\Delta s \approx \Gamma$. We cannot in fact distinguish between the channels that contribute to two intervals of the kinematic curve at s_1 and s_2 if $|s_2 - s_1| \leq \Gamma$. This is true when Γ is sufficiently small. In this case indeed one can consider as a straight segment the part of the curve contained between s_1 and s_2 . In this approximation the energy resolution in the RCS is given by

$$(16) \quad \Gamma_{j-k} = \left| \frac{dE_{j-k}}{ds} \right| \Gamma$$

From relations (9), (10) and (12) one has

$$(16') \quad \Gamma_{j-k} = \frac{M}{m_j + m_3} \left| 1 - c_i E_i^{-1/2} \right| \left| \frac{dE_i}{ds} \right| \Gamma$$

Fig. 8 reports as bases of the triangles the value of Γ_{j-k} . As one can see these values have the minima at the minimum value of E_{j-k} , that correspond to the zeros of dE_i/ds , that is to the inversion points.

4.2. - Angular resolution. -

From eqs. (13) results that the angular resolution in ϕ_{i-jk} is the same than the in ϕ_i in the LS, that is $\sim 1^\circ$ for the used geometry. The angular resolution in θ_{i-jk} does not differ appreciably from that in the θ_i , provided the total momentum is small with respect to the momenta of the detected particles in the LS. That in $\Delta\theta_{i-jk} \approx 1^\circ$.

There is on the contrary an amplification of the angular uncertainty in passing from the LS angles to the θ_{rel} and ϕ_{rel} . As relations (13) and (14) show, this amplification is proportional to $(\cos \theta_{rel})^{-1}$. Fig. 8 reports as error bars the angular resolution in θ_{rel} as a function of E_{j-k} .

4.3. - Distribution of pulses in the RCS and conclusions. -

As one can see from Fig. 8, the differential cross section $d^3\sigma / dE_{j-k} d\Omega_{i-jk} d\Omega_{rel}$ shows a peak at $E_{j-k} \approx 0.8 \pm 0.05$ MeV and the

peak energy does not vary with angles. The peak is asymmetric and the half-width at half maximum in the sense of increasing energy is $\Delta E_{1/2} = 0.6 \pm 0.1$ MeV as one measures in Fig. 8 for full curve peaks. This peak is the characteristic resonant peak of the ${}^5\text{He}$ ground state and its position and width are in good agreement with those reported in ref. (12) if one takes into account the energetic resolving power in the RCS for the present experiment.

The height of the peak varies with angles denoting a non-isotropic angular correlation between the two α -particles. The form of the peak is however rather constant, for the full curves in Fig. 8. The dashed curves, on the contrary are not in agreement with the full curves, at least in the high energy tail of the peak. This is to be expected because of the identity interference term in the LS density $N(s)$.

It is not possible to say from so few spectra neither the detailed angular correlation nor whether there are other contributions from other states of ${}^5\text{He}$ or from the ${}^8\text{Be}$ formation. This will be possible only when the other spectra in the LS will be examined.

For this reason it was not performed in this paper the transformation to the RCS which selects the neutron as the "first" emitted particle. This will be convenient when the contribution of the ${}^5\text{He}$ ground state to the reaction will be completely extracted from the data.

ACKNOWLEDGEMENTS. -

The authors would like to acknowledge Mr. G. Caruso, Mr. V. Scuderi, Mr. S. Pace and Mr. G. Panasci for their assistance during the experiments.

Grateful thanks are also due to Prof. C. Milone, Prof. G. Calvi and Prof. S. Notarrigo for the useful discussions.

REFERENCES. -

- (1) - J.L. Quebert and H. Sztark, Proc. Symp. on Heavy Ion Reactions, Saclay (1971); J. Physique suppl. 11-12, 255 (1972).
- (2) - C. Milone and R. Potenza, Nuclear Phys. 84, 25 (1966); R. Potenza, Proc. Intern. School "E. Fermi", XXXVI Course, Varenna (1965).
- (3) - L. Maranez, J.P. Langier, R. Ballini, C. Leweille, N. Samuer et J. Rey, Nuclear Phys. A97, 321 (1967); Y. Flamant, Y. Chanut et R. Ballini, J. Physique 28, 622 (1967).
- (4) - I. Duck, Revs. Modern. Phys. 37, 418 (1965); G.C. Phyllips, Revs. Modern. Phys. 37, 409 (1965); C.M. Jones, J.K. Bair, C.H. Johnson, H.P. Willard and M. Reeves, Revs. Modern Phys. 37, 437 (1965).
- (5) - G. Deconninck, A. Giorni, J.P. Longequeue, J.P. Maillard and T.U. Chan, Phys. Rev. C3, 2085 (1971).
- (6) - K. Bähr, T. Becker, O.M. Bilaniuk and R. Jahr, Phys. Rev. 178, 1706 (1969).
- (7) - V.K. Dolinov, Yu. V. Melikov, A.F. Tulinov and O.V. Bormot, Nuclear Phys. A129, 577 (1969).
- (8) - M. Jain, P.G. Roos, F.G. Pugh and H.D. Halmgren, Nuclear Phys. A153, 49 (1970).
- (9) - V.K. Dolinov, D.V. Meboniya and A.F. Tulinov, Nuclear Phys. A129, 597 (1969).
- (10) - F.B. Morinigo, Nuclear Phys. A127, 116 (1969); C.A. McMahan and I.M. Duck, Nuclear Phys. A157, 417 (1970).
- (11) - G.G. Olhson, Nuclear Instr. and Meth. 37, 240 (1965).
- (12) - G. Weber, Phys. Rev. 110, 529 (1958).
- (13) - C. Lanczos, Linear differential operators, (Van Nostrand, London, 1961), pag. 129-134.